2009

Electron-Induced Bond Breaking at Low Energies in HCOOH and Glycine: The Role of Very Short-Lived σ* Anion States

Gordon A. Gallup
University of Nebraska-Lincoln, ggallup1@unl.edu

Paul Burrow
University of Nebraska-Lincoln, pburrow1@unl.edu

Ilya I. Fabrikant
University of Nebraska-Lincoln, ifabrikant@unl.edu

Electron-induced bond breaking at low energies in HCOOH and glycine: The role of very short-lived σ^* anion states

Gordon A. Gallup, Paul D. Burrow, and Ilya I. Fabrikant
Department of Physics and Astronomy, University of Nebraska, Lincoln, Nebraska 68588-0111, USA
(Received 15 January 2009; published 1 April 2009)

Cross sections for dissociative electron attachment (DEA) to formic acid and glycine are calculated by the resonant *R*-matrix theory. A model with one effective reaction coordinate close to the O-H stretch motion is employed. The choice of the anion *R*-matrix pole and the surface amplitude as functions of the reaction coordinate for formic acid are based on scattering phase-shift calculations using the finite element discrete model. For glycine the input parameters are adjusted to reproduce experimental data. The results show that the mechanism of DEA in these molecules is similar to that for the hydrogen halides and involves electron capture into a σ^*(OH) orbital so that no σ^*/π^* coupling is required. Nonlocal effects play an important role for both molecules. In particular, pronounced steps and cusps are seen at the vibrational excitation thresholds. A sharp threshold peak in glycine is interpreted as a vibrational Feshbach resonance.

DOI: 10.1103/PhysRevA.79.042701 PACS number(s): 34.80.Ht

I. INTRODUCTION

Low-energy electron interactions with biological molecules in the gas phase have been proven to be a challenge for experimentalists and theorists alike. Although the field has been highly motivated by applications to radiation damage [1], it warrants fundamental interest because of the remarkable variety of bond-breaking reactions produced through the dissociative electron attachment (DEA) process,

$$e^- + AB \rightarrow A + B^-,$$

where the fragments A and B^- are not necessarily atomic. This arises not only from the properties of the initially formed temporary anion states, e.g., their symmetries, energies, lifetimes, and antibonding sites, but also from the range of neutral bond energies, dipole moments, and fragment electron affinities found in complex molecules. In addition, from a chemistry point of view, the theory of DEA produces insight into the fundamental electrochemical reduction process producing ions and radicals.

Progress in understanding interactions with large systems such as DNA strands and proteins must be grounded on an accurate analysis of the DEA process in the simplest components of these systems. Surprisingly, in the case of the amino acids and closely related molecules such as formic acid (HCOOH), there is not yet a consensus on the mechanism by which electrons with energies near 1.2 eV produce the sole fragment $(M\text{-H})^-$, where $(M\text{-H})$ represents the target molecule minus an H atom. In this work, we present a theoretical treatment of this process in the two compounds that have been studied most extensively, namely, HCOOH and glycine, the simplest of the amino acids. We show that the existing experimental results can be explained by invoking a single σ^* valence anion state in which the additional electron is largely located on the OH bond [2]. The calculated properties of this resonance in HCOOH are extreme, such that the resonance energy and width are very large, 5.3 and 5.8 eV, respectively. Such a short-lived anion state located at this energy would not *a priori* be expected to play a direct or substantial role in the low-energy DEA process. Indeed, almost all of the experimental studies have attributed the DEA process to initial electron attachment into the COOH π^* orbital followed by out-of-plane distortions that couple this orbital to σ^*(OH), ultimately producing the $(M\text{-H})^-$ fragment. This interpretation was also put forth in a theoretical study by Rescigno *et al.* [3].

The primary significance of the present work is thus to call attention to this class of very short-lived high-lying resonances whose large widths preclude their direct observation in the total electron-scattering cross section but which are clearly manifested, as we will show, in the DEA and vibrational excitation cross sections at much lower energies. Second, we show that in HCOOH and glycine, and, by implication, in the other amino acids as well, capture into the π^* orbital followed by π^*/σ^* coupling is not required to account for the bond breaking.

The temporary anion states of HCOOH [4–6], glycine, and several other amino acids [5] were first studied using electron transmission spectroscopy (ETS) [7]. Pronounced resonances in the total scattering cross sections near 1.9 eV were located in each compound and assigned to the occupation of the empty π^* orbital residing on the COOH group [5]. Subsequently, mass analysis of the anion fragments produced by DEA in this energy regime was carried out by a number of groups. A listing of these studies may be found in Ref. [6]. The common feature observed in this work was the production of $(M\text{-H})^-$ with a peak cross section near 1.2 eV, just above the estimated threshold energies at which these anions can be made. Above the peak, the cross sections fall relatively quickly as a function of increasing electron energy, and in measurements with higher-energy resolution, weak structure was also observed in the cross section. In the cases in which a resonance assignment was put forth, the authors ascribed the process as initiated by electron attachment into the empty π^* orbital residing on the COOH group. This choice was undoubtedly due to the close proximity of the π^* resonances to the DEA peaks and the absence of any other observed resonances in this energy regime.

Because of the planar geometry of HCOOH, the π^* temporary anion state cannot dissociate to $HCOO^- + H$ while re-

maining planar for reasons of symmetry. In their theoretical study of electron attachment to HCOOH, Rescigno *et al.* [3] showed that out-of-plane distortions can couple the initially formed π^* resonance with a σ^* anion state allowing the $(M\text{-H})^-$ fragment to be produced, and thus lending theoretical support to the π^* assignment. It is important to note, however, that this work did not calculate the actual DEA cross section but dealt only with possible anion surfaces along which the process might take place. We note that the σ^* and π^* resonances are one bond farther apart in HCOOH than in other planar systems where this interaction is properly invoked. In addition, the forces on the atoms are different, such that the out-of-plane (rotational) vibration of the O-H group in the π^* temporary anion still has a real frequency.

In a recent study of the total DEA cross sections of the amino acids by Scheer *et al.* [2], the arguments for invoking a single σ^* resonance were pointed out. It was noted that the peak cross sections for the production of $(M\text{-H})^-$ lie consistently 0.4–0.7 eV below the COOH π^* resonance energies, in contrast to other examples such as thymine, cytosine, and adenine, in which π^*/σ^* coupling has been invoked and certain peaks in the production of $(M\text{-H})^-$ do occur within experimental error at the energies of the π^* resonances [6]. This discrepancy in energy has also been noted independently by Vasil'ev *et al.* [8]. However, the most compelling argument for the role of a σ^*(OH) resonance is given by a study of vibrational excitation in HCOOH by Allan [9], who found that the cross section for excitation of the OH stretching mode declines slowly from its peak value near the vibrational threshold rather than peaking at the energy of the π^* resonance. He pointed out that this vibrational mode appears to be excited through a mechanism other than the π^* resonance and suggested that it could be related to a broad OH σ^* shape resonance. Allan noted as well the presence of cusplike features in the excitation functions for $\nu=1$ and 2 at the thresholds for excitation of higher levels of the OH stretching mode, and significantly, a dip in the DEA cross-section data of Pelc *et al.* [10] at the $\nu=4$ threshold. Each of these properties [11] is consistent with the existence of a broad σ^*(OH) shape resonance in HCOOH, and by extension, to the COOH group in the amino acids.

The purpose of the present study is to put these claims on a quantitative basis by showing that the essential features of the electron scattering in this energy range can be accounted for using a quasidiatomic model, allowing motion only along the OH stretching coordinate and a single σ^*(OH) anion potential function. We will compare our results with the DEA data of Pelc *et al.* [10] in HCOOH and the recent high-resolution study of glycine by Abouaf [12]. The calculations will be considered successful if a σ^* resonance can be found whose energy and width, as used in this model, can reproduce the shape, including sharp structures, and magnitudes of the DEA cross sections of glycine and HCOOH.

II. THEORY

For the DEA calculations we employ the resonance R matrix theory which starts with the one-pole approximation for the R matrix [13] representing the σ^* resonance in formic acid and glycine. In the fixed-nuclei approximation,

$$R(\{Q\}) = \frac{\gamma^2(\{Q\})}{W(\{Q\}) - E} + R_b, \tag{1}$$

where $\{Q\}=Q_1,Q_2,\ldots$ is the set of reaction coordinates, with Q_1 being the separation between the $(M\text{-H})$ complex and the H atom. The function $\gamma(\{Q\})$, called the R-matrix surface amplitude, determines the magnitude of the resonance width. R_b is a background term weakly dependent on $\{Q\}$ and the electron energy E, and $W(\{Q\})$ is the position of the fixed-nuclei R-matrix pole. It can be expressed in terms of the potential-energy surfaces for the neutral molecule $V(\{Q\})$ and the anion $U(\{Q\})$ as

$$W(\{Q\}) = U(\{Q\}) - V(\{Q\}). \tag{2}$$

To find the R-matrix parameters for HCOOH, we start with a calculation of the resonance-scattering phase shifts using the finite element discrete model (FEDM) method described by Nesbet [14] combined with an approximate version of the variational technique for quasi-bound-states developed by Froelich and Brandäs [15]. Hazi [16,17] made early calculations using the method without incorporation of the Froelich-Brandäs technique. The pseudocontinuum functions for our procedure involves s, p, and d states. Polarization interactions were included using both an effectively infinite order summation of first-order effects and an approximate second-order Møller-Plesset (MP) correction due to second-order effects. A least-squares correction of the temporary negative-ion singly-occupied orbital was used to prevent variational collapse of the quasi-bound-state of the underlying Feshbach resonance theory. We note that the "extreme" properties of the σ^* resonance alluded to in Sec. I were obtained this way for the vertical geometry.

To simplify the DEA treatment, we employ a one-dimensional model according to which the H dissociation occurs along the O-H bond coordinate, roughly corresponding to the normal O-H coordinate in the neutral molecule. This is, however, a substantial simplification; the problem is actually multidimensional. Our attempts to calculate the anion energy along the normal O-H coordinate resulted in a potential curve which is too repulsive and does not reproduce the threshold onset in DEA of HCOOH. We then calculated the curve corresponding to the minimum-energy dissociation path which turned out to be much less repulsive. In nonlocal DEA calculations the anion state is coupled with the vibrational states of the neutral molecule responsible for autodetachment. These were chosen as eigenstates of the nuclear Hamiltonian corresponding to the motion along the normal coordinate for O-H stretch vibrations. Of course, for a rigorous treatment, the multimode character of vibrations should be taken into account. However, the present problem requires a nonlocal treatment, and incorporation of multimode effects into nonlocal theory is still very difficult.

Although the present approach is not rigorous, it has the advantage of providing the correct positions of the threshold structures in the calculated scattering cross sections. To see this, we note that in the R-matrix formulation of the DEA

theory [18] the nonlocal complex potential for a given total energy E is constructed out of the generalized Franck-Condon factors $\gamma_{E\nu^-\nu}$ describing the capture of the incident electron by the molecule in the initial vibrational state ν into the dissociating state $E\nu^-$ and the logarithmic derivative L_ν of the electron wave function in each vibrational channel ν. For the polyatomic case, ν stands for all vibrational quantum numbers describing the initial state of the target and ν^- stands for all quantum numbers describing the final vibrational states of the fragments. The initial state ψ_ν can be expressed as a function of the normal coordinates $q_1, q_2, \ldots$ of the target and the final state as a function of the reaction coordinates $Q_1, Q_2, \ldots$, where, in the case of one dissociation path, Q_1 stands for the separation between the centers of mass of the fragments. Then the factor $\gamma_{E\nu^-\nu}$ is generally calculated as

$$\gamma_{E\nu^-\nu} = \int \psi_{E\nu^-}(Q_1, Q_2, \ldots)\gamma(Q_1, Q_2, \ldots)\psi_\nu(q_1(Q), q_2(Q), \ldots)dQ_1 dQ_2 \ldots, \tag{3}$$

where $q_1(Q), \ldots$ are the normal coordinates of the target expressed as functions of the reaction coordinates. In one-dimensional calculations we reduce Eq. (3) to a one-dimensional integral

$$\gamma_{E\nu} = \int \psi_E(\rho)\gamma(\rho)\psi_\nu(\rho)d\rho, \tag{4}$$

where ρ is an effective reaction coordinate and ν now stands for *one* vibrational quantum number representing the normal mode which is most strongly coupled with the dissociation channel. The choice of this mode requires an empirical input coming from observation of threshold features (steps and cusps) at vibrational excitation thresholds. In the R-matrix theory the threshold features are generated by the electron energy dependence of the logarithmic derivatives L_ν. For example, in a recent study [19] of DEA to the chloroform molecule, a cusp at the threshold for vibrational excitation of the symmetric deformation mode ν_3 was observed in experiment. This allowed us to choose a one-dimensional model where the dissociation channel is coupled with the ν_3 normal mode. Similarly, for formic acid and glycine it is natural to couple the dissociative motion to the normal vibration corresponding to the O-H stretch. Reducing Eq. (3) to Eq. (4) requires also some adjustment of the surface amplitude. As is well known, and will be demonstrated in the present paper, the DEA cross section is very sensitive to γ; therefore some additional empirical tunings of γ will be necessary to obtain the correct results for the DEA cross section.

In the present calculations we present the neutral and anion surfaces as functions of the effective coordinate ρ and parametrize them in the Morse form

$$V(\rho) = A(e^{\alpha\rho} - 1)^2, \quad U(\rho) = Be^{-2\beta\rho} - Ce^{-\beta\rho} + D. \tag{5}$$

To reproduce the value of the bond dissociation energy, 4.54 eV [20], and vibrational quantum, 0.44 eV for O-H stretch vibrations, for both glycine and formic acid, we chose initially $A=4.74$ eV and $\alpha=1.21$ a.u. However, the threshold features in DEA to glycine are better described by assuming vibrational quantum 0.43 eV. The corresponding parameter is $\alpha=1.182$. For the negative-ion curve we use the asymptotic value 1.42 eV for formic acid and 1.35 eV for glycine [21], which correspond to the DEA thresholds 1.20 and 1.13 eV, respectively.

The constants B, C, and β in Eq. (5) for formic acid were adjusted in the R-matrix approach to fit the *ab initio* FEDM calculations of resonance energies and phase shifts. Since the results of resonance energy calculations by the FEDM method do not exactly correspond to the R-matrix resonance poles, there is some arbitrariness in choosing the anion parameters. We have chosen them on the following basis: first, we adjust the resonance energy at R(O-H)=1.0 Å to the result of the FEDM calculation, 3.62 eV, and the curve asymptotic limit to the known values of the dissociation energy and electron affinity of the H atom. The parameters β and C were adjusted so that the anion curve was low enough in the crossing region. Raising $U(\rho)$ in this region by decreasing β or C leads to DEA cross sections which are too small. Although there is some arbitrariness in choosing β and

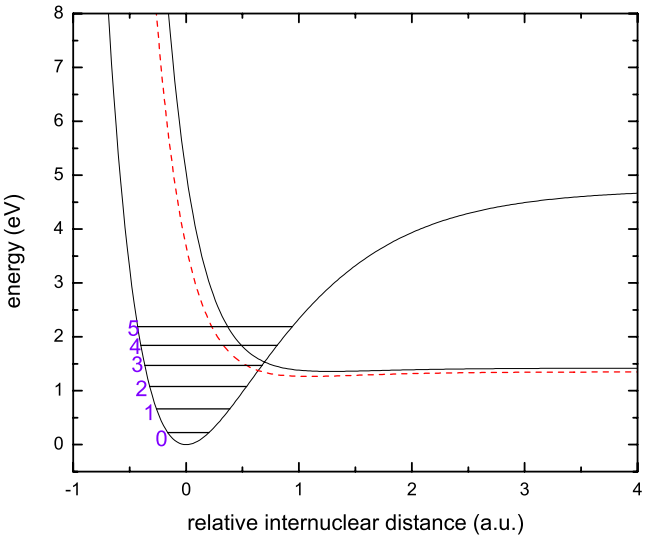

FIG. 1. (Color online) Potential-energy curves as functions of the effective reaction coordinate ρ (measured relative to the equilibrium internuclear separation). Vibrational energy levels are shown by horizontal lines. Anion curve—solid: formic acid; set 1—dashed: glycine. Note that the crossing point is $\rho=0.669$ a.u. for formic acid and 0.638 a.u. for glycine.

TABLE I. Anion curve parameters and vertical attachment energies for formic acid (FA) and glycine (G), sets 1 and 2.

Case	β (a_0^{-1})	B (eV)	C (eV)	D (eV)	VAE (eV)
FA	1.70	4.70	1.07	1.32	4.95
G 1	1.7	3.40	1.07	1.35	3.68
G 2	1.7	2.585	1.07	1.35	2.865

C, their choice, together with the choice of parameters for the surface amplitude γ, was ultimately based on the fitting to the resonance phase shifts.

For glycine we used essentially the same anion curve as for the formic acid with the asymptotic value $D=1.35$ eV. Since the polarizability of glycine is higher, we expect a lower vibrational excitation (VAE). On the other hand, since the resonance width is very large, the results for the cross sections are very insensitive to the exact value of $U(0)$ but rather to the value of $U(\rho)$ at the crossing point, $\rho=\rho_{\mathrm{cr}}$. In our calculations we have chosen two curves corresponding to $U(0)=3.68$ (set 1) and 2.865 eV (set 2). The results are summarized in Table I and Fig. 1.

The surface amplitude $\gamma(\rho)$ was represented in the form

$$\gamma(\rho) = \gamma_1 + \frac{\gamma_2}{e^{\eta\rho} + a}. \tag{6}$$

Parameters γ_1, γ_2, η, a, and R_b were adjusted to reproduce the energy dependence of the resonance phase shift calculated by the FEDM method. Since these phase shifts were calculated over a broad energy range, we were not successful in fitting them with an energy-independent background. Instead, we used a linear approximation for R_b in Eq. (1),

$$R_b = R_0 + ER_1. \tag{7}$$

It also appeared that a better fit to the *ab initio* phase shifts can be obtained with the following parametrization:

$$\gamma(\rho) = \gamma_1 + \frac{\gamma_2}{1 + b\rho}. \tag{8}$$

DEA calculations for glycine serve mostly for illustrative purposes, and the parameter choice was largely empirical. The choice of the R-matrix parameters is summarized in Table II. Set 1 for formic acid corresponds to the exponential parametrization, Eq. (6), and set 2 to the rational parametrization, Eq. (8).

In Figs. 2 and 3 we present comparisons of the fitted resonance phase shifts for formic acid with the results of the FEDM calculations. Both models demonstrate a good fit except in the low-energy region where a substantial disagreement is observed, particularly at the equilibrium O-H separation. We should note at this point that formic acid has a substantial dipole moment close to the critical value $d_{\mathrm{cr}}=0.6395$ a.u. at $R(\mathrm{O\text{-}H})=R_e=0.9695$ Å. According to our Hartree-Fock+MP2 calculations, at this distance it equals 0.539 a.u., which agrees quite well with the experimental value, 0.525 a.u. It grows quickly with an increase in R(O-H) reaching 0.887 a.u. at $R(\mathrm{O\text{-}H})=1.2$ Å. According to the general theory of the threshold behavior [22], the resonance width as a function of the electron wave number k behaves as

$$\Gamma = \mathrm{const}\frac{|k^{2\lambda+1}|}{|\xi - ie^{-i\pi\lambda}k^{2\lambda+1}|^2}, \tag{9}$$

where ξ is a parameter depending on the short-range interaction and λ depends only on the dipole moment d. For $d<d_{\mathrm{cr}}$, λ is real and $-0.5<\lambda<0$. For $d>d_{\mathrm{cr}}$, $\lambda=-0.5+i\mu$, where μ is real.

The R-matrix calculations incorporate the electron-dipole interaction exactly; therefore they demonstrate the correct threshold behavior of Γ and the resonance phase shift. In contrast, it is not clear to what extent the dipole effects are incorporated in the FEDM calculations; therefore deviations in the low-energy region are not surprising.

After the fixed-nuclei R-matrix parameters are determined, the vibrational dynamics is incorporated by inclusion of a nuclear kinetic-energy operator in the R matrix [23] in the quasiclassical approximation [18,24,25]. The strong dependence of dynamical capture and decay amplitudes is due to the long-range (dipolar and polarization) interaction which is included in the electron part of the problem. The geometry-dependent dipole moment was used as discussed above. For glycine we used the experimental value 0.551 a.u. and assumed that it is geometry independent. For polarizabil-

TABLE II. R-matrix parameters (all in a.u.) for formic acid (FA), sets 1 and 2, and glycine (G), sets 1 and 2.

Set	γ_1	γ_2	η	a	b	R_0	R_1
FA 1	−0.078	5.989	3.596	6.954		0.8022	−6.474
FA 2	−0.078	0.8412			1.823	0.9733	−6.575
G 1	−0.069	3.278	2.358	3.436		1.754	0
G 2	−0.069	3.200	2.358	3.436		1.754	0

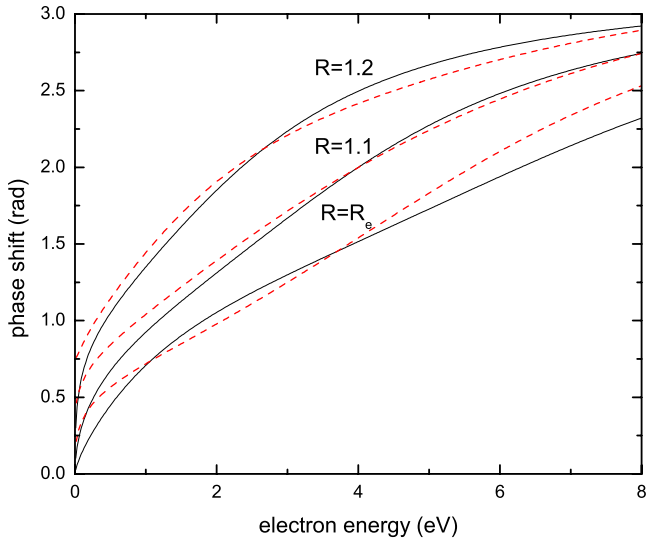

FIG. 2. (Color online) Resonant contribution to the scattering phase shift for formic acid for the internuclear distance $R=R_e=0.9695$, $R=1.1$, and $R=1.2$ Å. The corresponding values of the relative internuclear distance ρ (see Fig. 1) are 0, 0.247, and 0.436 a.u. FEDM calculations: solid lines; R-matrix results with exponential parametrization [Eq. (6)]: dashed lines.

ities we used the values 17.0 and 29.85 a.u. for formic acid and glycine, respectively, which were obtained using the PCGAMESS computation package [26,27].

III. RESULTS

A. Formic acid

In Fig. 4 we present the resonance width as a function of electron energy E for several internuclear separations. The width is growing fast with E and reaches very high (perhaps even unrealistically high) values for the equilibrium internuclear separation. What is remarkable, however, is that even

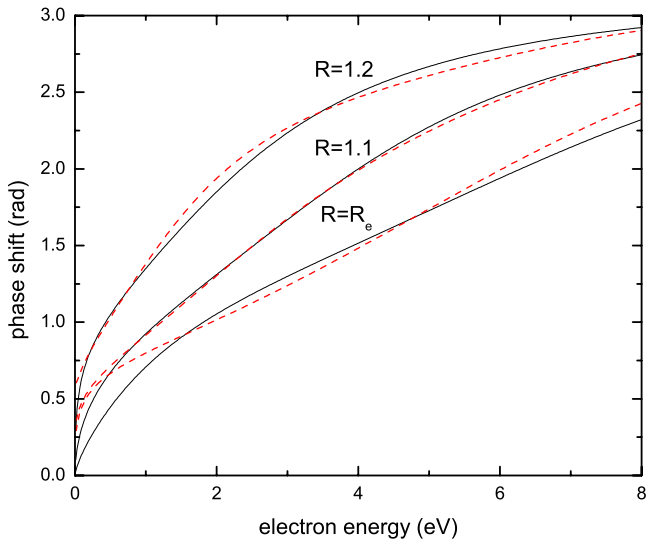

FIG. 3. (Color online) The same as in Fig. 2 but for the rational parametrization, Eq. (8).

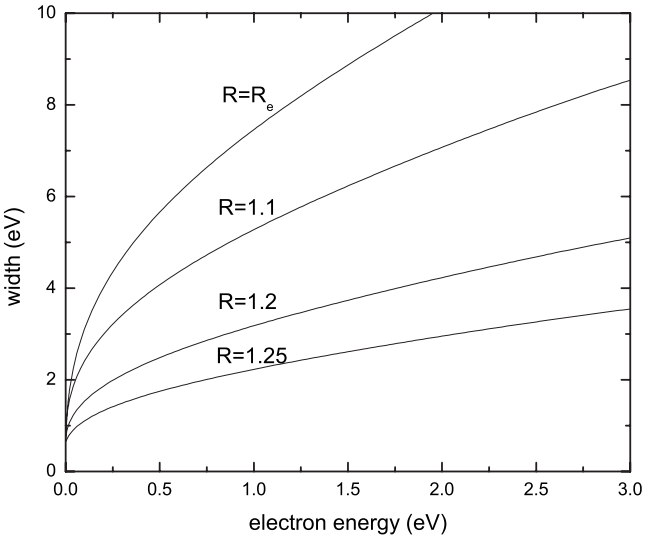

FIG. 4. The resonance width for HCOOH as a function of energy for the internuclear distance $R=R_e=0.9695$, $R=1.1$, $R=1.2$, and $R=1.25$ Å. The corresponding values of the relative internuclear distance ρ (see Fig. 1) are 0, 0.247, 0.436, and 0.530 a.u.

such a high width generates non-negligible DEA cross sections. Apparently for the DEA dynamics, the region of nuclear geometries close to the crossing point is more important than the equilibrium position.

In Fig. 5 we present DEA cross sections for formic acid. Pronounced cusps appear at the $\nu=3$, $\nu=4$, and $\nu=5$ thresholds. The calculation with the exponential parametrization for γ gives a sharp peak at the $\nu=3$ threshold and agrees better with the experiment [10]. In the second model, with the rational parametrization, γ is substantially bigger to the left of the equilibrium separation and somewhat bigger in the curve-crossing region. Due to this, the DEA cross section is substantially suppressed near the threshold. Comparison of

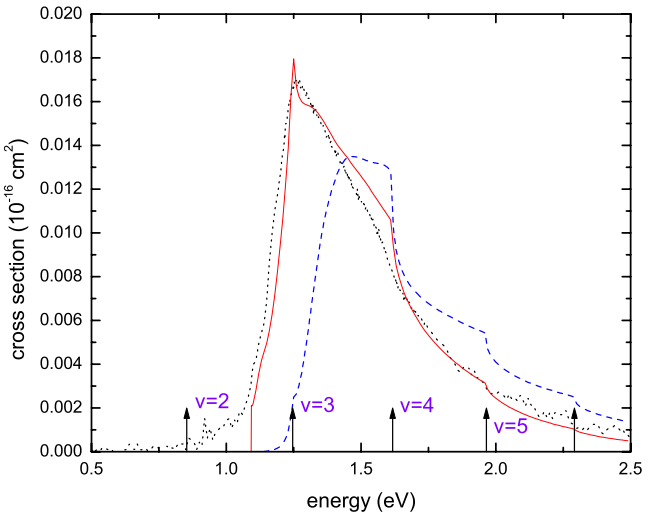

FIG. 5. (Color online) DEA cross section for formic acid. Solid curve: theory with exponential parametrization for γ; dashed curve: theory with the rational parametrization for γ. Dotted curve: experimental data [10]. Thresholds for vibrational excitation of O-H vibrations are indicated by arrows.

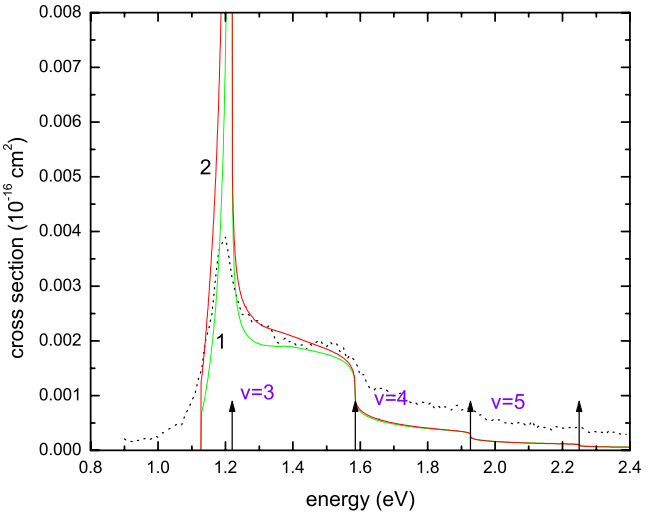

FIG. 6. (Color online) DEA cross section for glycine. Solid curves marked as 1 and 2 are calculations of sets 1 and 2, respectively, Dotted curve: experimental results [12] normalized to 0.002 Å^2 at 1.4 eV. Thresholds for vibrational excitation of O-H vibrations are indicated by arrows.

the two calculations demonstrate how sensitive the DEA cross sections are to the resonance width (which is proportional to γ^2). Additional calculations with a more repulsive anion curve show a poorer agreement with the experiment. Overall, the DEA cross-section shape is very close to that observed for hydrogen halides [25,28,29], although the more gradual rise at the DEA threshold does not look exactly like the vertical onsets in hydrogen halides.

B. Glycine

For glycine we used an empirical approach, employing the relative DEA cross section of Abouaf [12] and scaling it to 0.002 Å^2 at 1.4 eV [2]. The experimental estimate for the peak value of the DEA cross section for glycine is 0.004 Å^2 [2], but since the threshold peak is very sharp, this value can be affected by the experimental energy resolution. With our normalization, the magnitude of the computed cross section at the peak is 0.015 Å^2.

In Fig. 6 we present DEA cross sections for glycine. The experimental data of Abouaf [12] show a very sharp peak just below the $\nu(\mathrm{OH})=3$ threshold which is reproduced quite well by our calculations. The position of the peak is at $E=1.217$ and 1.213 eV in the calculations of sets 1 and 2, respectively, whereas the vibrational excitation threshold with our model parameters is at $E=1.220$ eV. This allows us to interpret the peak as a vibrational Feshbach resonance (VFR) [11]. Although the dipole moment of glycine is subcritical, a relatively large polarizability leads to the VFR formation. This feature makes the glycine case different from the hydrogen halides but similar to CH_3I whose dipole moment is also subcritical, but a VFR is observed [30]. According to the Abouaf data [12], the same feature is observed for *d* alanine. The down-step structure at the $\nu(\mathrm{OH})=4$ threshold agrees quite well with Abouaf's data, although we do not have, of course, the structure at the $\nu(\mathrm{OH})=3+\nu(\mathrm{CN})$ threshold, observed by Abouaf, because we do not include CN vibrations in our model.

IV. CONCLUSION

The present calculations confirm the experimental observations [2,9,12] suggesting that the low-energy DEA to HCOOH and glycine occurs through a $\sigma^*(\mathrm{OH})$ resonance and does not require the σ^*/π^* coupling. In spite of the fact that the σ^* resonance in these systems is extremely broad, our results are not entirely surprising because of their similarities with results for hydrogen halides [25,28,29,31–33].

The important part of the present calculations allowing us to reproduce threshold features is the use of the nonlocal complex potential approach [28] or the equivalent resonance *R*-matrix approach [18]. The resonance position and width at the equilibrium internuclear geometry are very large. From the point of view of the local theory, these parameters would not lead to a noticeable DEA cross section. However, according to Figs. 1 and 4, the position and width vary by almost 1 order of magnitude even within the Franck-Condon region. Therefore no conclusion should be made regarding the efficiency of the DEA process by looking at the resonance parameters at the equilibrium molecular geometry alone.

Since the implementation of the nonlocal theory in polyatomic cases is still quite challenging, in the present calculations we have used a one-dimensional model. However, to get a higher-quality *ab initio* results, further development of the nonlocal theory would be certainly necessary.

ACKNOWLEDGMENTS

We thank Paul Scheier and Robert Abouaf for providing their respective data sets. I. I. F. was supported by the National Science Foundation under Grant No. PHY-0652866.

[1] L. Sanche, Eur. Phys. J. D **35**, 367 (2005).
[2] A. M. Scheer, P. Mozejko, G. A. Gallup, and P. D. Burrow, J. Chem. Phys. **126**, 174301 (2007).
[3] T. N. Rescigno, C. S. Trevisan, and A. E. Orel, Phys. Rev. Lett. **96**, 213201 (2006).
[4] M. Tronc, M. Allan, and F. Edard, *Proceedings of the Fifteenth International Conference on the Physics of Electronic and Atomic Collisions*, edited by J. Geddes, H. B. Gilbody, A. E. Kingston, C. J. Latimer, H. R. J. Walters (ICPEAC, Brighton, 1987), p. 335.
[5] K. Aflatooni, B. Hitt, G. A. Gallup, and P. D. Burrow, J. Chem. Phys. **115**, 6489 (2001).
[6] K. Aflatooni, A. M. Scheer, and P. D. Burrow, J. Chem. Phys. **125**, 054301 (2006).

[7] L. Sanche and G. J. Schulz, Phys. Rev. A **5**, 1672 (1972).
[8] Y. V. Vasil'ev, B. J. Figard, D. F. Barofsky, and M. L. Deinzer, Int. J. Mass. Spectrom. **268**, 106 (2007).
[9] M. Allan, J. Phys. B **39**, 2939 (2006).
[10] A. Pelc, W. Sailer, P. Scheier, N. J. Mason, E. Illenberger, and T. D. Märk, Vacuum **70**, 429 (2003); A. Pelc, W. Sailer, P. Scheier, and T. D. Märk, *ibid.* **78**, 631 (2005).
[11] H. Hotop, M.-W. Ruf, M. Allan, and I. I. Fabrikant, Adv. At., Mol., Opt. Phys. **49**, 85 (2003).
[12] R. Abouaf, Chem. Phys. Lett. **451**, 25 (2008).
[13] A. M. Lane and R. G. Thomas, Rev. Mod. Phys. **30**, 257 (1958).
[14] R. K. Nesbet, Phys. Rev. A **24**, 1184 (1981).
[15] P. Froelich and E. Brandäs, Phys. Rev. A **12**, 1 (1975).
[16] A. U. Hazi, J. Phys. B **11**, L259 (1978).
[17] A. U. Hazi, in *Electron-Molecule and Photon-Molecule Collisions*, edited by T. N. Rescigno, V. McKoy, and B. Schneider (Plenum, New York, 1978).
[18] I. I. Fabrikant, Phys. Rev. A **43**, 3478 (1991).
[19] J. Kopyra, I. Szamrej, K. Graupner, L. M. Graham, T. A. Field, P. Sulzer, S. Denifl, T. D. Märk, P. Scheier, I. I. Fabrikant, M. Braun, M.-W. Ruf, and H. Hotop, Int. J. Mass. Spectrom. **277**, 130 (2008).
[20] A. Pelc, W. Sailer, P. Scheier, M. Probst, N. J. Mason, E. Illenberger, and T. D. Märk, Chem. Phys. Lett. **361**, 277 (2002).
[21] S. Gohike, A. Rosa, E. Illenberger, F. Brüning, and M. A. Huels, J. Chem. Phys. **116**, 10164 (2002).
[22] I. I. Fabrikant, Zh. Eksp. Teor. Fiz. **73**, 1317 (1977) [Sov. Phys. JETP **46**, 693 (1977)].
[23] M. LeDourneuf, B. I. Schneider, and P. G. Burke, J. Phys. B **12**, L365 (1979).
[24] S. A. Kalin and A. K. Kazansky, J. Phys. B **23**, 4377 (1990).
[25] I. I. Fabrikant, S. A. Kalin, and A. K. Kazansky, J. Chem. Phys. **95**, 4966 (1991).
[26] A. V. Nemukhin, B. L. Grigorenko, and A. A. Granovsky, Moscow Univ. Chem. Bull. (Engl. Transl.) **45**, 75 (2004).
[27] M. W. Schmidt, K. K. Baldridge, J. A. Boatz, S. T. Elbert, M. S. Gordon, J. H. Jensen, S. Koseki, N. Matsunaga, K. A. Nguyen, S. J. Su, T. L. Windus, M. Dupnis, and J. A. Montgomery, J. Comput. Chem. **14**, 1347 (1993).
[28] W. Domcke, Phys. Rep. **208**, 97 (1991).
[29] I. I. Fabrikant, S. A. Kalin, and A. K. Kazansky, J. Phys. B **25**, 2885 (1992).
[30] A. Schramm, I. I. Fabrikant, J. M. Weber, E. Leber, M.-W. Ruf, and H. Hotop, J. Phys. B **32**, 2153 (1999).
[31] J. Horáček and W. Domcke, Phys. Rev. A **53**, 2262 (1996).
[32] G. A. Gallup, Y. Xu, and I. I. Fabrikant, Phys. Rev. A **57**, 2596 (1998).
[33] M. Čižek, J. Horáček, and W. Domcke, Phys. Rev. A **60**, 2873 (1999).